Proc. Natl. Acad. Sci. USA
Vol. 90, pp. 10962–10966, December 1993
Biochemistry

Conversion of α-helices into β-sheets features in the formation of the scrapie prion proteins

(cellular prion protein/protein conformation/secondary structure/amyloid/post-translational modification)

KEH-MING PAN*, MICHAEL BALDWIN*, JACK NGUYEN*, MARIA GASSET*†, ANA SERBAN*, DARLENE GROTH*, INGRID MEHLHORN*, ZIWEI HUANG*‡, ROBERT J. FLETTERICK‡§, FRED E. COHEN‡§¶, AND STANLEY B. PRUSINER*§‖

Departments of *Neurology, §Biochemistry and Biophysics, ‡Pharmaceutical Chemistry, and ¶Medicine, University of California, San Francisco, CA 94143

Contributed by Stanley B. Prusiner, August 10, 1993

ABSTRACT **Prions are composed largely, if not entirely, of prion protein (PrP^{Sc} in the case of scrapie). Although the formation of PrP^{Sc} from the cellular prion protein (PrP^{C}) is a post-translational process, no candidate chemical modification was identified, suggesting that a conformational change features in PrP^{Sc} synthesis. To assess this possibility, we purified both PrP^{C} and PrP^{Sc} by using nondenaturing procedures and determined the secondary structure of each. Fourier-transform infrared (FTIR) spectroscopy demonstrated that PrP^{C} has a high α-helix content (42%) and no β-sheet (3%), findings that were confirmed by circular dichroism measurements. In contrast, the β-sheet content of PrP^{Sc} was 43% and the α-helix 30% as measured by FTIR. As determined in earlier studies, N-terminally truncated PrP^{Sc} derived by limited proteolysis, designated PrP 27–30, has an even higher β-sheet content (54%) and a lower α-helix content (21%). Neither PrP^{C} nor PrP^{Sc} formed aggregates detectable by electron microscopy, while PrP 27–30 polymerized into rod-shaped amyloids. While the foregoing findings argue that the conversion of α-helices into β-sheets underlies the formation of PrP^{Sc}, we cannot eliminate the possibility that an undetected chemical modification of a small fraction of PrP^{Sc} initiates this process. Since PrP^{Sc} seems to be the only component of the "infectious" prion particle, it is likely that this conformational transition is a fundamental event in the propagation of prions.**

Prions are proteinaceous infectious particles that are composed largely, if not entirely, of an abnormal isoform of the prion protein (PrP) designated, in the case of scrapie, PrP^{Sc} (1). Prions cause four neurodegenerative diseases of humans and six of animals, including scrapie of sheep and bovine spongiform encephalopathy. That the human prion diseases are manifest as infectious, familial, and sporadic disorders posed an enigma until it was discovered that mutations in the PrP gene are genetically linked to development of neurodegeneration (2).

PrP^{Sc} is synthesized from the normal cellular isoform PrP^{C} by a post-translational process that probably occurs in endosomes (3–6). Attempts to identify a post-translational chemical modification that features in the conversion of PrP^{C} into PrP^{Sc} have been unsuccessful (7). These findings raised the possibility that PrP^{Sc} differs from PrP^{C} only with respect to conformation. Many properties of PrP^{Sc} differ from those of PrP^{C}: (*i*) PrP^{Sc} is insoluble in detergents, while PrP^{C} is readily solubilized under nondenaturing conditions (8); (*ii*) PrP^{Sc} is partially hydrolyzed by proteases to form a fragment designated PrP 27–30, while PrP^{C} is completely degraded under the same conditions (9); (*iii*) PrP^{Sc} accumulates, whereas PrP^{C} turns over rapidly (3); and (*iv*) the patterns of PrP^{Sc} accumulation in brain are distinct from the distribution of PrP^{C} (10).

The protease-resistant core of PrP^{Sc} designated PrP 27–30 polymerizes into rod-shaped structures which are indistinguishable from many purified amyloids both ultrastructurally and tinctorially (11). In the brains of some, but not all, animals and humans that have died of prion diseases, amyloid plaques are found which contain PrP, as determined by immunostaining and Edman protein sequencing studies (12–14). That PrP 27–30 polymerizes into amyloid suggests that it might have a β-pleated sheet structure (11), since all amyloids studied, to date, have been found to have this structure (15). About 50% of the secondary structure of PrP 27–30 is β-sheet, as measured by Fourier-transform infrared (FTIR) spectroscopy (16, 17), a percentage that is much higher than that predicted from the amino acid sequence (18). Two-thirds of the β-sheet content of PrP 27–30 is low-frequency (LF) β-sheet, which often reflects intermolecular associations that are a characteristic of amyloids (17). The LF β-sheet content of PrP 27–30 declined upon denaturation under conditions that diminished scrapie infectivity (17). Disruption of the amyloid polymers composed of PrP 27–30 by dispersion into liposomes altered neither the LF β-sheet content nor prion infectivity (19).

Computational analyses of a family of homologous PrP sequences suggested that PrP^{C} might be folded into a four-helix bundle (20). When the four putative α-helices were synthesized as peptides, three of the four polymerized into amyloid fibrils with ≈70% of the secondary structure LF β-sheet (20). Other investigators have also demonstrated polymerization of synthetic PrP peptides into amyloid (21–23).

To examine the possibility that formation of PrP^{Sc} involves the conversion of α-helices in PrP^{C} into β-sheets, we developed a PrP^{C} purification protocol utilizing nondenaturing procedures. As reported here, we determined the secondary structures of both PrP^{C} and PrP^{Sc}. Our findings suggest that the fundamental event in the formation of PrP^{Sc} as well as propagation of prion infectivity is the conversion of α-helices in PrP^{C} into β-sheets.

MATERIALS AND METHODS

All chemicals were of the highest grade commercially available. $^{2}H_{2}O$ was purchased from Aldrich; nondenaturing detergents, including Zwittergent 3-12 (ZW), were from Calbiochem; SDS was from BDH; proteinase K was from Beckman;

The publication costs of this article were defrayed in part by page charge payment. This article must therefore be hereby marked "*advertisement*" in accordance with 18 U.S.C. §1734 solely to indicate this fact.

Abbreviations: PrP, prion protein; PrP^{c}, cellular PrP; PrP^{Sc}, scrapie PrP; PrP 27–30, protease-resistant fragment of PrP^{Sc}; FTIR, Fourier-transform infrared; LF, low-frequency; mAb, monoclonal antibody; ZW, Zwittergent 3-12; WGA, wheat germ agglutinin; EM, electron microscopy.

†Present address: Departmento Bioquimica, Universidade Complutense, 28040 Madrid, Spain.

‖To whom reprint requests should be addressed at: Department of Neurology, HSE-781, University of California, San Francisco, CA 94143-0518.

and guanidine hydrochloride was from Pierce. *N*-Acetylglucosamine, 3-(*N*-morpholino)propanesulfonic acid (Mops), and 2-(*N*-morpholino)ethanesulfonic acid (Mes) were obtained from Sigma. Anti-PrP monoclonal antibody (mAb) 3F4 was kindly provided by Richard Kascsak (Institute of Basic Research, Staten Island, NY).

Syrian golden hamsters (Lak:LVG) were purchased from Charles River Breeding Laboratories. For PrP^C purification, the animals were sacrificed at 12 weeks of age by CO_2 asphyxiation. Brains were removed immediately, frozen in liquid N_2, and stored at −80°C until use. Propagation of prions and production of PrP^{Sc} in Syrian hamsters have been described (11).

Purification of PrP^C (24) was modified to avoid using low pH, urea, and SDS/PAGE, all of which might denature PrP^C. A crude microsomal fraction was prepared from 100 normal hamster brains, extracted with ZW, and centrifuged at 100,000 × *g* for 1 hr. The supernatant was applied to an IMAC-Cu^{2+} column (Pharmacia), which was washed with 5 vol of 0.015 M imidazole/0.15 M NaCl/10 mM sodium phosphate, pH 7.0/0.2% ZW. PrP^C was eluted by increasing the imidazole to 0.15 M. The pH of the eluate was adjusted to 6.4 with 2 M HCl prior to loading onto an SP Sepharose cation-exchange column (1.5 × 3 cm) that had been equilibrated with 0.15 M NaCl/20 mM Mes, pH 6.4/0.2% ZW. The column was washed with 20 mM Mops, pH 7.0/0.2% ZW (buffer A) containing initially 0.15 M NaCl and then 0.25 M NaCl. PrP^C was eluted with buffer A containing 0.5 M NaCl. The eluate was concentrated and desalted on an IMAC-Co^{2+} column (1 × 2.5 cm), from which PrP^C was eluted with 0.1 M imidazole in buffer B (0.15 M NaCl/20 mM Mops, pH 7.5/0.2% ZW) and applied to a wheat germ agglutinin (WGA)-Sepharose (Vector Laboratories) column (1 × 6.5 cm) equilibrated in the same buffer. The flow rate was 0.3 ml/min during loading, then 0.75 ml/min. After washing with 10 vol of buffer B, PrP^C was eluted by 0.05 M *N*-acetylglucosamine in buffer B. Purified PrP^C fractions were pooled and concentrated with a Centricon-30 (Amicon). *N*-Acetylglucosamine was removed by three washes in 0.15 M NaCl/10 mM sodium phosphate, pH 7.5/0.12% ZW (PBSZ) and samples were stored at −20°C.

Purifications of PrP 27–30 and PrP^{Sc} from scrapie-infected Syrian hamster brains have been described (11, 25). PrP^{Sc} and PrP 27–30 (0.5 mg) were washed and centrifuged (100,000 × *g* for 1 hr) three times with PBSZ and once with ^2H_2O/PBSZ. The final pellet was resuspended into 0.15 ml of ^2H_2O/PBSZ by sonication.

Proteins were denatured in sample buffer by boiling for 3 min and analyzed by SDS/PAGE (12% acrylamide) (26). Resolved proteins on the gel were visualized by silver staining (27). For immunoblotting proteins were electrophoretically transferred onto Immobilon-P membrane (Millipore) (28). After transfer, the membrane was blocked at 37°C for 1 hr with 5% nonfat dry milk in 0.15 M NaCl/10 mM Tris·HCl, pH 8.0/0.05% Tween-20 (TBST). Subsequently, it was incubated with anti-PrP 13A5 mAb (29) in TBST overnight and then alkaline phosphatase-conjugated secondary antibody (Promega) for 90 min at room temperature. Immunoreactive material was stained with 5-bromo-4-chloro-3-indolyl phosphate (BCIP) and nitro blue tetrazolium (NBT). Amino acid analysis was carried out as described previously (30).

Samples for FTIR were dissolved or dispersed in ^2H_2O/PBSZ and equilibrated at least 18 hr and analyzed in a transmission cell having CaF_2 windows and a 50-μm path length. Proteins and buffer were analyzed under identical conditions in a Perkin–Elmer System 2000 FTIR spectrophotometer at 2-cm^{-1} resolution. Difference spectra were obtained by interactive subtraction. Smoothing and Fourier self-deconvolution were applied to increase the spectral resolution in the amide I′ region (1700–1600 cm^{-1}) and then least-squares iterative curve fitting to Lorentzian line shapes was carried out. The proportion of each secondary structural element was computed as described previously (17, 31). CD of PrP^C in PBSZ was measured in an Aviv Associates 62 DS spectropolarimeter at 25°C under constant nitrogen flush in a quartz cell with a 0.1-cm path length. The instrument was calibrated by using *d*-(+)-10-camphorsulfonic acid.

Electron microscopy (EM) of PrP 27–30 has been described previously (11). Protein samples were diluted to 10–50 μg/ml in PBSZ; pioloform resin (0.8%) and carbon-coated 400-mesh nickel grids were floated on one drop of this solution for 1 min then washed three times with water. The grids were blocked with phosphate-buffered saline/0.8% bovine serum albumin/0.1% gelatin (buffer C) for 15 min, then incubated with anti-PrP 3F4 mAb (1:100 dilution in buffer C) for 30 min. Excess anti-PrP 3F4 mAb was removed by four washes with buffer C. Gold particle (5 nm) conjugated goat antibody to mouse IgG (EY Laboratories) diluted 1:50 in buffer C was applied for 30 min. The grids were washed four times in buffer C and twice in water and were negatively stained with uranyl formate for 10 s (32, 33). Electron micrographs were obtained by using a JEOL 100CX electron microscope at 80 keV.

RESULTS

The final step in the PrP^C purification utilized lectin chromatography (Fig. 1 *Upper*) based on earlier observations that PrP 27–30 binds to WGA (34). The extent of enrichment relative to other proteins was evaluated by SDS/PAGE and silver-staining. Fractions 52–57 (pool 2) eluted from the WGA-Sepharose gave only a single band of 33–35 kDa (Fig. 1 *Lower*, lane c) and bound anti-PrP 13A5 mAb (lane f).

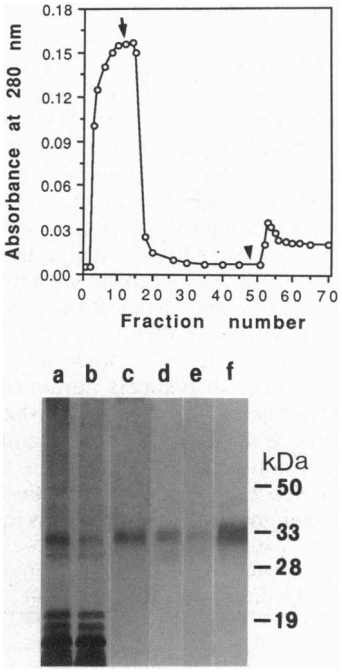

FIG. 1. Purification and analysis of PrP^C. (*Upper*) Elution of PrP^C from WGA-Sepharose. The 0.1 M imidazole eluate from IMAC-Co^{2+} was applied to a WGA column. The arrow indicates wash with buffer B; the arrowhead indicates the start of 50 mM *N*-acetylglucosamine in buffer B. Fractions of 1.5 ml each were pooled as follows: 4–15 gave pool 1, 52–57 gave pool 2. (*Lower*) SDS/PAGE with the proteins stained with silver (lanes a–c) or transferred to an Immobilon membrane and immunostained with anti-PrP 13A5 mAb (lanes d–f). Lanes a and d, eluate from IMAC-Co^{2+}; lanes b and e, pool 1; lanes c and f, pool 2.

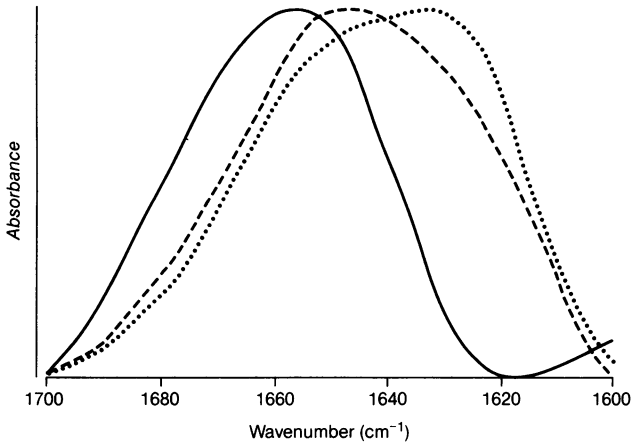

FIG. 2. FTIR spectroscopy of prion proteins. The amide I′ band (1700–1600 cm^{-1}) of transmission FTIR spectra of PrP^{C} (solid line), PrP^{Sc} (dashed line), and PrP 27–30 (dotted line) is shown. These proteins were suspended in $^{2}H_{2}O$ ($D_{2}O$) containing 0.15 M NaCl, 10 mM sodium phosphate at pD 7.5 (uncorrected), and 0.12% ZW. The spectra are scaled independently to be full scale on the ordinate axis (absorbance).

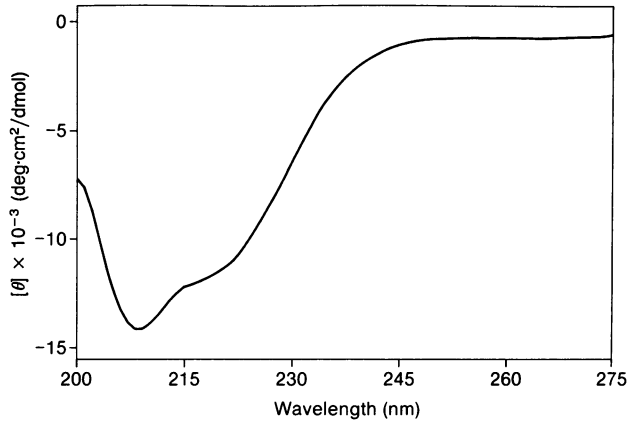

FIG. 3. CD of PrP^{C}. Purified PrP^{C} was prepared in 0.15 M NaCl/10 mM sodium phosphate, pH 7.5/0.12% ZW. The ordinate axis (molar ellipticity [θ]) was calibrated by using amino acid analysis to measure amount of protein.

The amide I′ band of the FTIR spectrum of purified PrP^{C} from pool 2 showed a symmetrical peak with a maximum at 1653 cm^{-1} (Fig. 2, solid line). Such spectra are characteristic of proteins with high α-helix content. In contrast, the FTIR spectra of PrP^{Sc} (Fig. 2, dashed line) and PrP 27–30 (Fig. 2, dotted line) showed patterns which are characteristic of proteins with high β-sheet content. Deconvolution of the PrP^{C} spectrum gave an estimate of 42% α-helical content and only 3% β-sheet, whereas the PrP^{Sc} and PrP 27–30 spectra revealed 43% and 54% β-sheet, respectively (Table 1). The secondary structure of PrP 27–30 determined here by transmission FTIR is in very good agreement with data from attenuated total reflection of thin films (17).

The secondary structures of PrP^{C} and PrP^{Sc} (residues 23–231) and PrP 27–30 (residues 90–231) were predicted by using a neural network algorithm (35, 36). Class-dependent (α/α, α/β, β/β) and naive predictions were performed (Table 1). The α/α class contains proteins which are composed largely of α-helices. Similarly, β/β class contains proteins that are mostly β-sheets. Interestingly, the four putative α-helices of PrP (20) showed both strong helix preference in the α/α class prediction and strong β-sheet preference in the β/β class prediction. These results are consistent with the hypothesis that these domains undergo conformational changes from α-helices to β-sheets during the formation of PrP^{Sc}. All of the predicted values for total α-helix plus β-sheet were less than those determined spectroscopically.

The FTIR spectrum for PrP^{C}, with a peak at 1653 cm^{-1}, is indicative of a secondary structure with a high α-helix content, and we sought confirmation of this interpretation by CD, a technique that gives an unambiguous signal for proteins with a large α-helical component. The CD spectrum of PrP^{C} shows a minimum at 208 nm and a shoulder at 222 nm, clearly indicating that the protein contains one or more α-helices (Fig. 3). For estimating the α-helical content of proteins, far UV data is thought to be preferable; however, the α-helical content can be determined from the ellipticity at 222 nm. At the 222-nm minimum the rotational strength of an amino acid polymer composed completely of α-helices varies depending on the helix length (37). The ellipticity data in Fig. 3 rely on a protein concentration determined by amino acid analysis. Assuming an average helix length of 14 residues, this gives an α-helix content of approximately 36% for PrP^{C}. No CD measurements were made for PrP^{Sc} or PrP 27–30 because of their insolubility, although CD spectra of these proteins deposited as thin films have been obtained (38).

By EM both PrP^{C} and PrP^{Sc} appeared as amorphous aggregates when dried onto grids (Fig. 4 *A* and *B*); the presence of these proteins was confirmed by immunogold labeling with anti-PrP 3F4 mAb. In contrast, polymers of PrP 27–30 were visualized as rod-shaped amyloid (Fig. 4*C*) (11). Amyloid polymers composed of PrP 27–30 have a higher proportion of LF β-sheet than PrP^{Sc}; the LF β-sheet characteristic of the intermolecular bonding associated with polymer formation is more pronounced for PrP 27–30.

DISCUSSION

From the studies reported here, we conclude the formation of PrP^{Sc} involves the conversion of α-helices in PrP^{C} into β-sheets (Table 1), but we cannot eliminate the possibility that an undetected chemical modification of a small fraction of PrP^{Sc} initiates this process. This conformational transition

Table 1. Secondary structure determinations from deconvolution and curve fitting to the FTIR amide I′ bands compared with predicted values

	Content of secondary structure, %										
	PrP						PrP 27–30				
	FTIR		Predicted*				FTIR	Predicted*			
Structure	PrP^{C}	PrP^{Sc}	Naive	α/α	α/β	β/β		Naive	α/α	α/β	β/β
α-Helix	42	30	14	31	27	0	21	20	45	39	0
β-Sheet	3	43	6	0	1	24	54	8	0	1	30
Turn	32	11					9				
Coil	23	16					16				

*Predicted values were calculated by using a neural network program (35). For PrP^{C} and PrP^{Sc} residues 23–231 were used in the calculation; for PrP 27–30 residues 90–231 were used. See text for description of the four types of prediction.

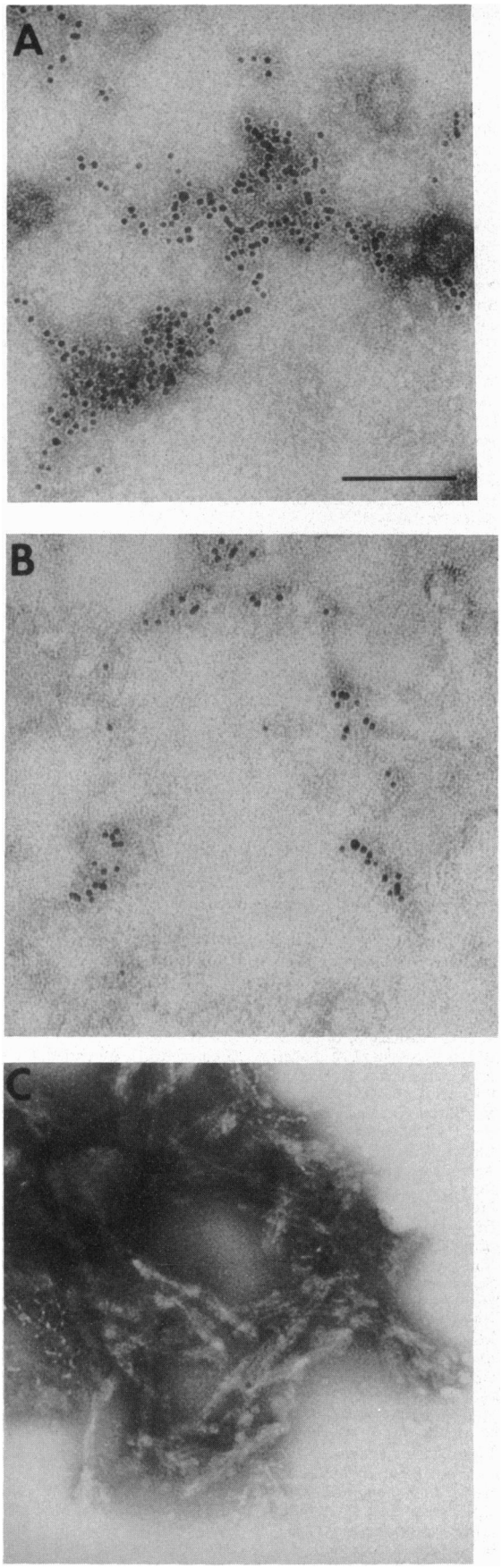

FIG. 4. Electron micrographs of negatively stained and immunogold-labeled PrPs. (*A*) PrP^{C}. (*B*) PrP^{Sc}. (*C*) Prion rods composed of PrP 27–30, negatively stained. (Bar = 100 nm.)

seems likely to be the fundamental molecular event that underlies prion propagation, since many lines of evidence argue that PrP^{Sc} is an essential component of infectious prion particles (1).

Since the accumulation of PrP^{Sc} seems to be responsible for the neurodegeneration found in prion diseases, we also conclude that the conversion of α-helices in PrP^{C} into β-sheets is likely to be the primary lesion in these illnesses. This assertion is supported by the finding that ablation of the PrP gene is apparently not deleterious to mice; thus, the prion diseases appear to be the result of PrP^{Sc} accumulation rather than a PrP^{C} deficiency (39). PrP^{Sc} accumulation is restricted to specific regions of the central nervous system and it is only these regions which exhibit vacuolation and reactive gliosis (10, 40–42). The foregoing findings lend further support to the argument that prion diseases are disorders of protein conformation.

It seems likely that PrP^{Sc} synthesis is a complex process, since all attempts to produce PrP^{Sc} in cell-free systems have been unsuccessful, to date (43). Metabolic radiolabeling studies with scrapie-infected cultured cells demonstrate that inhibition of protein synthesis during the chase period abolishes PrP^{Sc} formation (5). These findings argue that the continuing synthesis of proteins other than PrP^{C} is necessary for PrP^{Sc} production. It will be of considerable interest to learn which proteins participate in this process; presumably, such proteins catalyze the unfolding of the α-helices in PrP^{C} and the refolding of these domains into β-sheets as PrP^{Sc} is formed. These auxiliary proteins might be expected to share some properties with chaperones, which are known to facilitate protein folding (1, 44, 45).

Transgenetic studies have demonstrated that prion propagation is a highly specific process in which inoculated prions containing PrP^{Sc} trigger the synthesis of homologous prions from the homologous PrP^{C} (46, 47). While the initial studies demonstrating the specificity of prion formation were performed with transgenic mice expressing Syrian hamster PrP, similar results have been obtained with a chimeric mouse/Syrian hamster PrP transgene. Prions produced from transgenic mice with mouse/hamster PrP display artificial properties. Mice homozygous for ablation of the PrP gene ($Prnp^{0/0}$) are resistant to prion infection and do not propagate prions (48, 49).

Some investigators have suggested that scrapie agent multiplication proceeds through a crystallization process involving PrP amyloid formation (23, 50, 51). Although PrP amyloid plaques are diagnostic of prion diseases when present, they are often absent from both humans and animals with such diseases. Since PrP amyloid does not seem to be required for either propagation of prion infectivity or pathogenesis of disease and amyloid-like polymers have not been identified in cultured cells chronically synthesizing prions, we conclude that polymerization of PrP molecules is not necessary for prion synthesis (46, 52, 53). Furthermore, purified infectious preparations isolated from scrapie-infected hamster brains exist as amorphous aggregates (Fig. 4*B*); only if PrP^{Sc} is exposed to detergents and limited proteolysis does the protease-resistant core of PrP^{Sc} (PrP 27–30) polymerize into prion rods (Fig. 4*C*) exhibiting the ultrastructural and tinctorial features of amyloid (11, 53). Furthermore, dispersion of prion rods into detergent–lipid–protein complexes results in a 10- to 100-fold increase in scrapie titer, and no rods have been identified in these fractions by EM (19).

Examples of other proteins with α-helices that are converted into β-sheets and vice versa include the photosystem II reaction center, which exhibits an α-helix → β-sheet transition when exposed to light (54); gp120 from human immunodeficiency virus type I which possesses a β-sheet in aqueous environments that is converted into an α-helix when the virus binds to the membrane protein CD4 (55); and the

Serpin proteins, in which a β-sheet is transformed into an α-helix upon proteolytic activation (56). In Alzheimer disease, amyloid plaques contain βA4 peptide which is derived from amyloid precursor protein (β-APP) that seems to undergo a similar structural transition. βA4 is high in β-sheet content (51, 57, 58) but is proteolytically cleaved from a region of β-APP, a portion of which is thought to form a transmembrane α-helix (59).

While α-helical → β-sheet transitions feature in the formation of PrP^{Sc} and thus seem to be the fundamental events underlying prion "infection," the existence of scrapie "strains" remains perplexing (60). Prion "strains" produce distinct patterns of PrP^{Sc} deposition in the brain and often have different incubation times (40–42). In the continuing absence of any scrapie-specific nucleic acid, the profound conformational changes which PrP^{C} undergoes during its conversion to PrP^{Sc} raise the possibility that the information carried in prion "strains" resides within the conformation of PrP^{Sc} (1). The transitions in PrP structure underscore the concepts that (*i*) prion diseases are disorders of protein conformation and (*ii*) prions are a class of infectious pathogens which are different from viruses, viroids, bacteria, and fungi (61).

We thank Drs. Susan Fisher, Alan Frankel, and W. Curtis Johnson, Jr., for their help, Drs. Eric Goormaghtigh and Anthony Fink for advice concerning FTIR, and Dr. Alma Burlingame for his careful review of the manuscript. This work was supported by research grants from the National Institutes of Health as well as by gifts from the Sherman Fairchild Foundation, National Medical Enterprises, and the Bernard Osher Foundation.

1. Prusiner, S. B. (1991) *Science* **252,** 1515–1522.
2. Hsiao, K., Baker, H. F., Crow, T. J., Poulter, M., Owen, F., Terwilliger, J. D., Westaway, D., Ott, J. & Prusiner, S. B. (1989) *Nature (London)* **338,** 342–345.
3. Borchelt, D. R., Scott, M., Taraboulos, A., Stahl, N. & Prusiner, S. B. (1990) *J. Cell Biol.* **110,** 743–752.
4. Borchelt, D. R., Taraboulos, A. & Prusiner, S. B. (1992) *J. Biol. Chem.* **267,** 6188–6199.
5. Taraboulos, A., Raeber, A. J., Borchelt, D. R., Serban, D. & Prusiner, S. B. (1992) *Mol. Biol. Cell* **3,** 851–863.
6. Caughey, B. & Raymond, G. J. (1991) *J. Biol. Chem.* **266,** 18217–18223.
7. Stahl, N., Baldwin, M. A., Teplow, D. B., Hood, L., Gibson, B. W., Burlingame, A. L. & Prusiner, S. B. (1993) *Biochemistry* **32,** 1991–2002.
8. Meyer, R. K., McKinley, M. P., Bowman, K. A., Braunfeld, M. B., Barry, R. A. & Prusiner, S. B. (1986) *Proc. Natl. Acad. Sci. USA* **83,** 2310–2314.
9. Oesch, B., Westaway, D., Wälchli, M., McKinley, M. P., Kent, S. B. H., Aebersold, R., Barry, R. A., Tempst, P., Teplow, D. B., Hood, L. E., Prusiner, S. B. & Weissmann, C. (1985) *Cell* **40,** 735–746.
10. Taraboulos, A., Jendroska, K., Serban, D., Yang, S.-L., DeArmond, S. J. & Prusiner, S. B. (1992) *Proc. Natl. Acad. Sci. USA* **89,** 7620–7624.
11. Prusiner, S. B., McKinley, M. P., Bowman, K. A., Bolton, D. C., Bendheim, P. E., Groth, D. F. & Glenner, G. G. (1983) *Cell* **35,** 349–358.
12. Roberts, G. W., Lofthouse, R., Allsop, D., Landon, M., Kidd, M., Prusiner, S. B. & Crow, T. J. (1988) *Neurology* **38,** 1534–1540.
13. Kitamoto, T., Tateishi, J., Tashima, I., Takeshita, I., Barry, R. A., DeArmond, S. J. & Prusiner, S. B. (1986) *Ann. Neurol.* **20,** 204–208.
14. Tagliavini, F., Prelli, F., Ghisto, J., Bugiani, O., Serban, D., Prusiner, S. B., Farlow, M. R., Ghetti, B. & Frangione, B. (1991) *EMBO J.* **10,** 513–519.
15. Glenner, G. G., Eanes, E. D., Bladen, H. A., Linke, R. P. & Termine, J. D. (1974) *J. Histochem. Cytochem.* **22,** 1141–1158.
16. Caughey, B. W., Dong, A., Bhat, K. S., Ernst, D., Hayes, S. F. & Caughey, W. S. (1991) *Biochemistry* **30,** 7672–7680.
17. Gasset, M., Baldwin, M. A., Fletterick, R. J. & Prusiner, S. B. (1993) *Proc. Natl. Acad. Sci. USA* **90,** 1–5.
18. Bazan, J. F., Fletterick, R. J., McKinley, M. P. & Prusiner, S. B. (1987) *Protein Eng.* **1,** 125–135.
19. Gabizon, R., McKinley, M. P. & Prusiner, S. B. (1987) *Proc. Natl. Acad. Sci. USA* **84,** 4017–4021.
20. Gasset, M., Baldwin, M. A., Lloyd, D., Gabriel, J.-M., Holtzman, D. M., Cohen, F., Fletterick, R. & Prusiner, S. B. (1992) *Proc. Natl. Acad. Sci. USA* **89,** 10940–10944.
21. Forloni, G., Angeretti, N., Chiesa, R., Monzani, E., Salmona, M., Bugiani, O. & Tagliavini, F. (1993) *Nature (London)* **362,** 543–546.
22. Goldfarb, L. G., Brown, P., Haltia, M., Ghiso, J., Frangione, B. & Gajdusek, D. C. (1993) *Proc. Natl. Acad. Sci. USA* **90,** 4451–4454.
23. Come, J. H., Fraser, P. E. & Lansbury, P. T., Jr. (1993) *Proc. Natl. Acad. Sci. USA* **90,** 5959–5963.
24. Pan, K.-M., Stahl, N. & Prusiner, S. B. (1992) *Protein Sci.* **1,** 1343–1352.
25. Turk, E., Teplow, D. B., Hood, L. E. & Prusiner, S. B. (1988) *Eur. J. Biochem.* **176,** 21–30.
26. Laemmli, U. K. (1970) *Nature (London)* **227,** 680–685.
27. Merril, C. R., Dunau, M. L. & Goldman, D. (1981) *Anal. Biochem.* **110,** 201–207.
28. Towbin, H., Staehelin, T. & Gordon, J. (1979) *Proc. Natl. Acad. Sci. USA* **76,** 4350–4354.
29. Bolton, D. C., Seligman, S. J., Bablanian, G., Windsor, D., Scala, L. J., Kim, K. S., Chen, C. J., Kascsak, R. J. & Bendheim, P. E. (1991) *J. Virol.* **65,** 3667–3675.
30. Stahl, N., Borchelt, D. R. & Prusiner, S. B. (1990) *Biochemistry* **29,** 5405–5412.
31. Goormaghtigh, E., Cabiaux, V. & Ruysschaert, J.-M. (1990) *Eur. J. Biochem.* **193,** 409–420.
32. Williams, R. C. (1977) *Proc. Natl. Acad. Sci. USA* **74,** 2311–2315.
33. McKinley, M. P., Braunfeld, M. B., Bellinger, C. G. & Prusiner, S. B. (1986) *J. Infect. Dis.* **154,** 110–120.
34. Haraguchi, T., Fisher, S., Olofsson, S., Endo, T., Groth, D., Tarantino, A., Borchelt, D. R., Teplow, D., Hood, L., Burlingame, A., Lycke, E., Kobata, A. & Prusiner, S. B. (1989) *Arch. Biochem. Biophys.* **274,** 1–13.
35. Presnell, S. R., Cohen, B. I. & Cohen, F. E. (1993) *Comput. Appl. Biosci.* **9,** 373–374.
36. Kneller, D. G., Cohen, F. E. & Langridge, R. (1990) *J. Mol. Biol.* **214,** 171–182.
37. Yang, J. T., Wu, C.-S. C. & Martinez, H. M. (1986) *Methods Enzymol.* **130,** 208–269.
38. Safar, J., Roller, P. P., Gajdusek, D. C. & Gibbs, C. J., Jr. (1993) *J. Biol. Chem.* **268,** 20276–20284.
39. Büeler, H., Fischer, M., Lang, Y., Blüthmann, H., Lipp, H.-L., DeArmond, S. J., Prusiner, S. B., Aguet, M. & Weissmann, C. (1992) *Nature (London)* **356,** 577–582.
40. DeArmond, S. J., Yang, S.-L., Lee, A., Bowler, R., Taraboulos, A., Groth, D. & Prusiner, S. B. (1993) *Proc. Natl. Acad. Sci. USA* **90,** 6449–6453.
41. Hecker, R., Taraboulos, A., Scott, M., Pan, K.-M., Torchia, M., Jendroska, K., DeArmond, S. J. & Prusiner, S. B. (1992) *Genes Dev.* **6,** 1213–1228.
42. Casaccia-Bonnefil, P., Kascsak, R. J., Fersko, R., Callahan, S. & Carp, R. I. (1993) *J. Infect. Dis.* **167,** 7–12.
43. Raeber, A. J., Borchelt, D. R., Scott, M. & Prusiner, S. B. (1992) *J. Virol.* **66,** 6155–6163.
44. Martin, J., Langer, T., Boteva, R., Schramel, A., Horwich, A. L. & Hartl, F.-U. (1991) *Nature (London)* **352,** 36–42.
45. Liautard, J.-P. (1991) *FEBS Lett.* **294,** 155–157.
46. Prusiner, S. B., Scott, M., Foster, D., Pan, K.-M., Groth, D., Mirenda, C., Torchia, M., Yang, S.-L., Serban, D., Carlson, G. A., Hoppe, P. C., Westaway, D. & DeArmond, S. J. (1990) *Cell* **63,** 673–686.
47. Scott, M., Groth, D., Foster, D., Torchia, M., Yang, S.-L., DeArmond, S. J. & Prusiner, S. B. (1993) *Cell* **73,** 979–988.
48. Büeler, H., Aguzzi, A., Sailer, A., Greiner, R.-A., Autenried, P., Aguet, M. & Weissmann, C. (1993) *Cell* **73,** 1339–1347.
49. Prusiner, S. B., Groth, D., Serban, A., Koehler, R., Foster, D., Torchia, M., Burton, D., Yang, S.-L. & DeArmond, S. J. (1993) *Proc. Natl. Acad. Sci. USA* **90,** 10608–10612.
50. Gajdusek, D. C. & Gibbs, C. J., Jr. (1990) in *Biomedical Advances in Aging*, eds. Goldstein, A. (Plenum, New York), pp. 3–24.
51. Jarrett, J. T. & Lansbury, P. T., Jr. (1993) *Cell* **73,** 1055–1058.
52. McKinley, M. P., Taraboulos, A., Kenaga, L., Serban, D., Stieber, A., DeArmond, S. J., Prusiner, S. B. & Gonatas, N. (1991) *Lab. Invest.* **65,** 622–630.
53. McKinley, M. P., Meyer, R., Kenaga, L., Rahbar, F., Cotter, R., Serban, A. & Prusiner, S. B. (1991) *J. Virol.* **65,** 1440–1449.
54. He, W.-Z., Newell, W. R., Harris, P. I., Chapman, D. & Barber, J. (1991) *Biochemistry* **30,** 4552–4559.
55. Reed, J. & Kinzel, V. (1993) *Proc. Natl. Acad. Sci. USA* **90,** 6761–6765.
56. Mottonen, J., Strand, A., Symersky, J., Sweet, R. M., Danley, D. E., Geoghegan, K. F., Gerard, R. D. & Goldsmith, E. J. (1992) *Nature (London)* **355,** 270–273.
57. Hilbich, C., Kisters-Woike, B., Reed, J., Masters, C. L. & Beyreuther, K. (1991) *J. Mol. Biol.* **218,** 149–163.
58. Fraser, P. E., Nguyen, J. T., Surewicz, W. K. & Kirschner, D. A. (1991) *Biophys. J.* **60,** 1190–1201.
59. Kang, J., Lemaire, H.-G., Unterbeck, A., Salbaum, J. M., Masters, C. L., Grzeschik, K.-H., Multhaup, G., Beyreuther, K. & Muller-Hill, B. (1987) *Nature (London)* **325,** 733–736.
60. Dickinson, A. G., Meikle, V. M. H. & Fraser, H. (1968) *J. Comp. Pathol.* **78,** 293–299.
61. Prusiner, S. B. (1982) *Science* **216,** 136–144.